Pakistan Journal of Engineering and Technology
ISSN (Print): 2664-2042; ISSN (Online): 2664-2050
Received: 2023-06-14
Accepted: 2024-04-24
https://doi.org/10.51846/vol7iss2pp79-96

PAKJET
Pakistan Journal of Engineering & Technology

Article

A Critical Analysis of Design for Reduction in Vibrations of Centrifugal Impellers

Muhammad Umair Najeem, Syed Irtiza Ali Shah, and Majid Mehmood

Department of Mechanical Engineering, Air University Islamabad, Islamabad 44000, Pakistan
* Correspondence: Muhammad Umair Najeem (muhammadumairnajeem938@email.com)

Abstract: Centrifugal pumps are widely used for various applications. Numerous technical practices use centrifugal pumps, particularly when consistent and adaptable pump performance is required. Still, these can have several issues, including low efficiency when operated under off-design conditions and poor capitalization performance. These frequent transport mixtures, such as liquid and gas, and pure liquids. It is a well-known fact that several problems encountered by pumps in a pumping station are related to structural instability or impeller/blade failure. Vibrations can cause catastrophic failures in the impeller, so these must be kept to a minimum while designing the impeller. Vibration, cavitation, rough running, lower-than-expected efficiency, and shorter pump life can all be traced back to unfavorable process flow conditions. Although there are some design guidelines for pump configuration, the effects of fluctuating discharge on structural stability have yet to be investigated. An additional pressing problem is the identification of time cracks. Failure can occur due to cracks much before the design loads. In this work, we aim to investigate and analyze the centrifugal impeller design consideration. Using different methods for designing and modeling, we compared significant results and found the optimal solutions in which a centrifugal impellor can be designed. This work enables us to determine the best techniques and methods to overcome the problem of vibrations produced in the centrifugal impeller. This also helps us to understand the centrifugal pump's behavior and performance to improve its efficiency. Centrifugal impellors are compared across conditions, including free, forced, damped, and undamped systems. Three successful methods for designing and modeling a centrifugal impellor are proposed using these parameters. The methods of design and analysis provide predictions of the flow fields that are highly reliable. Regarding fluid distribution and pump efficiency, computational fluid dynamics provides various solutions that may be applied to impeller design. Using fluent software, we can better comprehend the pump's resonant operation. Blade mistuning is a severe problem that can be handled using the blade tip timing and strain gauge technique. Vibration and motor current signature analysis (MCSA) is also mentioned to investigate vibrational problems with the centrifugal impeller. Several strategies are discussed to lessen or eliminate the issue of vibrations in impellers. The limitations and disadvantages of using these techniques are discussed. The summary of results provides significant design and improvement in centrifugal pumps in the recent past.

Keywords: Centrifugal Impellers, Mistuning, Pump Configuration, Single Degree of Freedom System, Vibrations.

1. Introduction

1.1. Background and Motivation

The centrifugal pump is essential in many engineering and domestic applications, and many centrifugal pumps have one or more impellers attached to the rotary pump shaft. The arrangement of impellors and rotary pump shaft is used to conduct fluid through the pump system and piping.

Conversion of energy takes place using the impellors. The pump has dynamic mechanical energy. This energy is converted to energy of moving fluid using impellors. Energy is converted to kinetic as well as potential energy. In the opening cycle, fluid is directed to the suction ports with the help of the pump, and after that, it is guided towards the impellor's inlet. Pump liquid is moved along the spinning vanes while the velocity of the fluid is increasing at the same time.

After that, fluid is 'charged' and leaves the impeller vanes. High fluid velocity is generated when 'charged' fluid is conducted to diffuser casing, and this high fluid velocity is converted to high fluid pressure. In the end, a discharge port is used to transport the fluid for high-pressure fluid, and then it's on to the next stage of the multi-stage pumping system. Compressors benefited from the pump in the 19th and early 20th centuries as pumps were the leading knowledge at that time. After 1945, the compressors had more knowledge, and pumped benefited from it. The hydraulic design of centrifugal pump impellor mainly benefited from the great studies made in the field of centrifugal force in the recent past about centrifugal impellor aerodynamics and airfoil design. The modern concept of aerodynamics is applied to increase the performance of centrifugal impellor parameters such as higher head per stage, good performing inducer, and good Stability. The transfer of these trends from aero to hydro for improvement purposes will continue until we reach the level where more economic improvement is impossible. The development of centrifugal compressors is critical since it is closely linked to the growth of gas turbines, steel, and mining sectors. The theory and function of gas turbines were known even when their necessary material and complete knowledge about the flow mechanism were unknown. John Barber was the one who patented the concept of the gas turbine back in 1791, and the gas turbine was based on reciprocating compressors [1]. Rateau was the first successful dynamic compressor in 1905, and it used a centrifugal impellor, but until the 1930s, the gas turbine was not successfully developed. In 1939, Brown Boveri, where Zurich hosted the Swiss National Exhibition, demonstrated the first sizeable gas turbine power plant. The first turbojet- powered flight took place in 1939 as well. As far as the efficiency and power ratio of the turbojet engine is concerned, the compressor must have a centrifugal impellor. In the Von OHAIN engine, a centrifugal impellor was used, and in the Whittle engine in 1939 and 1941, respectively. At the beginning of the 20th century, many manufacturers used centrifugal impellors in industrial compressors, but their performance was not very good. There is a variety of configurations of impellors. The non- clogging wear-resistant pump is shown in Fig. 1. They generally have a designed open rotary.

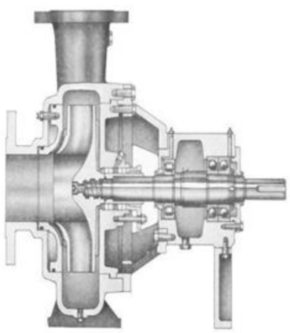

Figure 1. Process pump that is non-clogging and wear-resistant [2].

Now, let's look at the difference between a closed and an open impeller. A closed impellor has a front and back shroud, or two front shrouds 9, one on each side, in the case of a double suction impeller. This is the most essential and widely used option if maximal efficiency at the design point (BEP) is required. Fig. 2 shows a horizontal split case pump with double suction.

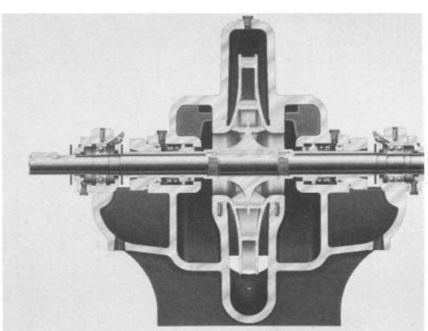

Figure 2. Pump with horizontal split casing and double suction [3].

The open impeller is found in the pulp and paper industry, as well as chemical and pharmaceutical services. The open impeller is shown in Fig. 3. An open impeller is always usedwhen a strangle material is fluid. It is widely used in this application as it can be cleaned. The back shroud area is tiny,if there is any. There is low axial thrust.

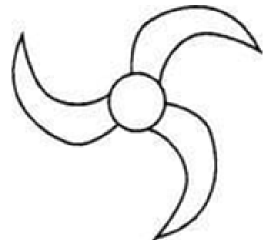

Figure 3. Open impeller [4].

Fig. 4 shows a semi-open (or semi-closed) impeller with a complete or partial back shroud. From wen reinforcement, it has a more robust blade design. When the back shroud increases, axial thrust increases until it is full; if a full shroud is utilized, it can handle stringy material and is easily cleaned.

Figure 4. The semi-open or semi-closed impeller [5].

The single suction impeller can be any of the above. It is the most commonly used impellor and has only one inlet. As the name indicates, the double-suction impellor has an inlet on both sides. It contains two single suction impellers that are symmetrical and back-to-back. There is an inherent balanced thrust condition in terms of non-symmetrical flow condition and non-symmetrical geometry condition in the impellor inlet, casing passages, and wear ring clearance.

1.2. Literature Review

After completing the design in 3D Vista, CPD was used to model the pump. The CFD simulation tool identifies the pressure distribution pattern and velocity profile. This research aims to look at a pump's impact and distribution of velocity profile and pressure with the following specifications: RPM = 1450, Head will be 20 m, and Flow rate will be 280 m^3/hr. Although experimental approaches and prior knowledge are crucial, Computational Fluid Dynamics is the most effective way to investigate pump performance (CFD). It has been discovered that the design and analysis methodologies produce extremely accurate flow field predictions. As a result, it is possible that the design can be improved to provide lower energy use, less head loss, increased flexibility, and longer component life [2].

A primary goal of the study is to provide a simulation of CFD. The simulation will be of a domestic centrifugal pump that does not require the involvement of methods based on mainly expansive experiments. Initially, the focus of this dissertation study will be on improving the head of currently available regenerative pumps. The impeller failure analysis is covered in the second part. The structural study of the impeller is included in the failure analysis. Structural analysis determines the impeller's total deformation and strain energy due to rotation. The analysis takes into consideration rotational velocity and hydrostatic pressure. The impeller is also subjected to solid-fluid interaction. The entire deformation of the impeller and the strain energy are calculated in structural analysis. The entire impeller's deformation and the impeller's strain energy are calculated using structural analysis. The impeller and casing dimensions were measured when the pump was dismantled. After that, the path of the flow and impeller were designed using the software CARIA V5. First, the flow of the pump and the impeller's structural analysis are verified. The paper's critical future scope is the likelihood of cavitation induced by the pump due to vapor formation in the fluid region and impeller. The impeller's total deformation and strain energy are determined using structural analysis [2], [6].

The study examines the current system, does CFD analysis for various discharge conditions, and conducts structural analysis. CFD and structural analysis of modified geometry. The main reason is the geometrical and hydraulic constraints unique to each site. Constructing a scaled model in the laboratory, observing the flow (via dye injection), and proposing changes to intake geometry are the most typical techniques for overcoming possible difficulties in new designs and fixing faults detected in existing installations. With rapid advances in Computational Fluid Dynamics (CFD),numerical simulation is now recognized as an efficient method for solving fluid issues due to cost and time constraints in modeling the distribution of flow and pressure inside the pump. By lowering the number of possibilities to be examined in a laboratory, it decreases the cost and time associated with finalizing the design of a pumping station. The best variant's time required for continual discharge will be determined during experimentation. A 1HP pump will be utilized in this procedure [7].

This paper entails a thorough examination of a centrifugal pump model, as well as the identification, observation, and CFD simulation tool that may determine the pattern of velocity profile and pressure distribution. This study will undoubtedly generate a wealth of helpful information while also contributing to our understanding of centrifugal pump design and features. For pump designers, CFD is a crucial tool. Today, CFD tools are widely used in the turbo-machinery business. Recent developments in processing power, rich visuals, and interactive 3D model manipulation have significantly reduced the time and expense of developing a CFD model and analyzing the results. Only after convergence is achieved are the results recorded. The pump impeller completed a full rotation while the solution iterated 1000 times. Contour maps are also obtained for static pressure, velocity, and wall shear stress distribution. As a result, the design and analysis methodologies produce extremely accurate flow field predictions. As a result, the approaches can be used to predict general performance. Before the prototype is created, the model can be adjusted to reduce energy consumption and heat loss, extend component life, and improve system adaptability [8].

Three-dimensional, Single, and two-phase flow CFD models of a centrifugal pump with closed and semi-open impellers are carried out. In a single-phase flow situation, the head prediction agrees satisfactorily with experimental results. A Eulerian-Eulerian mono-disperse appropriate combination with a quantitative turbulence model is used for two-phase flows. Because a bubble diameter more significant than the grid size prohibits finite volume grid cells from being refined further, a grid dependency is inescapable for enormous bubbles. Pump performance is being analyzed by air bubble diameter. A 2016 high-resolution camera is used to view and capture the flow details. ANSYS CEX is used for the simulation purpose disparity between simulation findings and measured data is lower than the grid sensitivity. Because measurements for the CI, a giant pump head is suggested than the OI, and the trailing edge is considered to have a negligible impact on upstream gas buildup, qualitative inferences it is presumed that two-phase flow is conceivable [8].

Centrifugal pump impeller geometry was formed in the ANSYS blade gen design modeler, then meshed in. At last, CFD analysis was conducted in ANSYS CFX using the ANSYS turbo grid meshing tool. The efficiency of the centrifugal pump is directly related tothe impeller area of exit. The Efficiency of a centrifugal pump improves as the impeller's exit diameter lowers. A centrifugal pump's performance improves as the impeller's trailing edge blade angle increases. The following are the findings reached as a result of all of the preceding cases. As the blade width at the impeller's exit rises, the pump impeller's performance improves in all of the previously mentioned criteria. As the length of the impeller's shroud reduces, the performance of the pump impeller improves in all parameters. The performance of the pump impeller improves as at the impeller's trailing edge, the blade angle (beta) increases [9].

Various factors can cause forced vibration of centrifugal compressor rotors that are not synchronous. Many are caused by aerodynamic events within the compressor's gas path. Typical flow disturbances that can induce forced vibration include stalling impellers, stalling diffusers, and flow problems induced by misalignment of an impeller and a diffuser. Thisconsisted mainly of, where appropriate, the use of CFD analytical data to characterize the flow. When available, the evaluation also includes dynamic pressure transducer test data that can beused to confirm the occurrence of such phenomena and data on rotor vibration indicating the occurrence of such phenomena. This contains actual machine test data that shows features like frequency and amplitude. Stalls in the impeller, diffuser, and interaction are some of the aerodynamic events contributing to increased radial vibrations. Flow physics was generally described, and the criteria for identifying each were used. Finally, numerous spectral frequencies and plots of waveforms in Fig. 5 were provided to show how different the various eventscan be seen on a spectrum analyzer or oscilloscope as vibration or pressure pulsationdata [10].

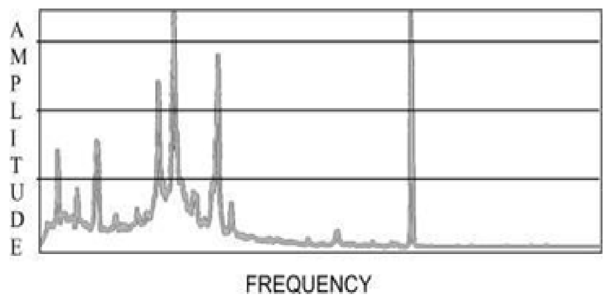

Figure 5. Frequency spectrum from periodic vibration signal of aerodynamics forces acting on centrifugal compressors [10].

This work looks into a new way of monitoring impeller conditions utilizing surface vibration and advanced signal analysis. It's critical to reduce noise to produce dependable and effective features since cavities and turbulences give overall vibration responses a high level of wideband noise. Vibration signals have two components. Mechanical and hydraulic pulsations have a more predictable discrete content, whereas flow turbulence and cavitation have a more random wideband content. A new approach for diagnosing defects in pump impellers is proposed in this research based on MSB vibrational analysis data. Because of its wideband noise suppression capability, MSB enables a more accurate estimation of spectral amplitude due to pulsations, as shown in Fig. 6 [11].

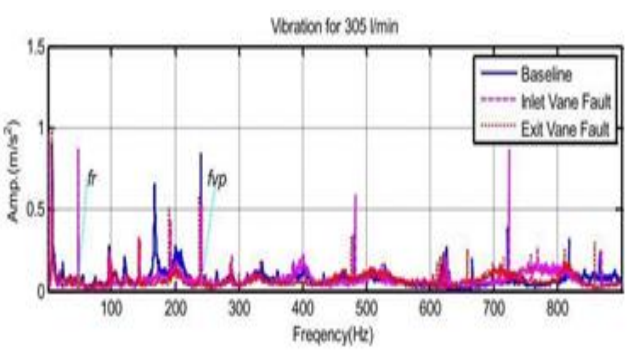

Figure 6. Vibration signals in the frequency domain [11].

A centrifugal pump having a large number of vaned diffusers, the fluctuation of the pressure of the impeller, and the vibration caused by the impellor was investigated in [12]. Within the operating condition of off-design, circumferentially, the pressure fluctuation on the impeller and its static volute pressure is unequal. Because of the fluctuations' circumferential unevenness, even when the rotor-stator interaction resonance requirement is not met, resonance can be stimulated, and sidebands appear in frequency spectra. Due to the inertia of water, the resonant frequency may be affected by the wave's traveling direction. The resonance of an impeller's nodal diameter mode is caused by the fluctuation of pressure acting upon the impeller, which can be stimulated even when theinteraction of rotor and stator, resonance requirement will not be satisfactory, as shown in in Fig. 7 [18]. Under cavitation and seal damage situations, a cyclostationary theory-based time-frequency signal analysis method is used to extract the frequency characteristics of non-stationary vibration signals [13]. The signal analysis was carried out first based on calculating CAFs (cyclic autocorrelation functions) for various signals. Furthermore, the findings regarding recognizing various typesof flaws may provide vital evidence to detect faults while the pump is running [13]. A sensor may be used to detect the commencement of thismechanism [14].

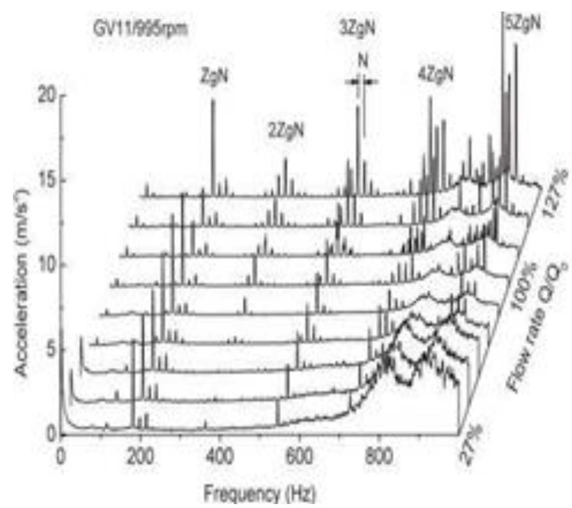

Figure 7. Vibration frequency spectra measured at Vd1on the hub of impeller Im^2 [12].

Impeller clogging phenomena in centrifugal pumps are a type of problem that causes the pumps to vibrate more and function less well. Furthermore, impeller obstruction may cause issues in the factory's production process. The purpose of this study is to use vibration and motor current analysis to detect a clogged impeller in a centrifugal pump. A test rig is used in this study, and the sealing tape clogs one of the impeller's passages. Clogging is detected using the Fast Fourier Transform based on vibration analysis (FFT). The finding demonstrates that the rotating frequency of the impeller is the dominating frequency in the impeller-clogging phenomena (1xRPM). The clogged impeller has more potent effects on axial vibration responses when vibration values are measured in three possible directions: horizontally, vertically, and axially. Furthermore, the electro motor's electrical current consumption is lowered in this circumstance. Because a piece of the impeller, like a clogged impeller, did not engage in fluid transfer and the flow rate dropped compared to a typical impeller, the electrical power consumption decreased accordingly, and their parameters are shown in Table 1 [15].

Table 1. Vibrations variation in three main directions [15].

First 6 harmonics	Horizontal	Vertical	Axial
1XPrimary	0/7	0/0.2	0/9
2XPrimary	0/1	0/0.3	0/0.5
3XPrimary	0/0.6	0/0.5	0/0.55
4XPrimary	0/1.6	0/1	0/0.1
5XPrimary	0/0.4	0/0.2	0/0.25
6XPrimary	0/0.5	0/0.1	0/0.05

Blade tip timing and strain gauge (BTT) measurements were used to elucidate the blade-forced vibration. Tip-timing further eliminates measurement-induced strain gauge mistuning and flow disruption. With the use of a parameter estimation method, the mistuning of the blade is recognized and quantified, and the numerical mistuned forced response model is updated. Finally, the blade's forced response was mistuned, demonstrating promising measurement agreement findings using the suggested BTT parameter-driven vibration prediction approach. This work has scientific value because it adds to our understanding of centrifugal fan blade vibration compressors utilizing tip- timing. It has industrial value because it considers mistuning issues using an efficient reduced-order modeling method [16].

The vibration of a centrifugal pump is first recorded in a healthy state and then compared to nine different sizes of artificial cracks put into the impeller blades. The results suggest that fault diagnosis, time index parameters, and frequency spectrum are useful. As the blade fracture size grows, the vibration time index and the amplitude of the impeller passing frequency both increase, which can be used as a defect severity indicator. Time and frequency domain vibration analysis was used to investigate impeller cracks in centrifugal pumps. Vibration is assessed in both healthy and unhealthy settings. The vibration index is used as a time-domain fault indication, and the power spectrum at specific frequencies is used as a frequency fault indicator. According to the findings, the vibration index rises as the size of the impeller crack increases. According to power spectrum research, the fundamental Frequency (impeller frequency) increases as the impeller fracture size increases. There are two harmonics of impeller frequency and sidebands of impeller rotation frequency, which are +45Hz and -45Hz, respectively [17].

Most industries rely on centrifugal pumps as a primary component. They are used to transport liquid through pipes in practically every sector. Pump failure results in significant production losses, so creating a cost- effective and user-friendly condition monitoring system is critical for promptly estimating a pump's condition and avoiding an unplanned failure. Invasive monitoring of the situation approaches established for pump problem detection rely on costly vibration sensors, which must be mounted for the data collection on the pump body. Although techniques that aren't intrusive have proven to be cost-effective, these are limited in their ability to diagnose incipient defects in pumps working in a loud industrial setting. Electric diagnostics technology (EDT) suggested in work [18] does not involve the acquisition of additional sensors; instead, it measures and displays the motor line current and voltage using the existing sensors that are often installed on machines.

The Design engineers face significant difficulty when it comes to operating machines in resonance bands. The research [19] investigates the vibrations of centrifugal fan casings, which are intense while the machine runs, especially in unstable situations. Fan casing vibrations with natural frequencies were determined through experiments based on experimental modal analysis. Additional numerical simulations aided in the establishment of theoretical values for the frequency of natural vibrations and their mode forms. The numerical model was changed after the findings were analyzed. The data was eventually applied to interpreting vibration measurements taken in real-world settings. The performance of a new nine-blade impeller was compared to that of an older eight-blade fan impeller. New solutions for casing operating beyond resonance frequencies and vibration zones have been developed. Vibrations measured in the casing in both steady and unstable states have the potential to produce damage, such as construction fractures. Casing vibrations at their natural frequencies occur with reduced amplitudeduring ordinary fan operation. The fan housing runs at resonance frequencies, as seen by high vibration natural frequencies levels of interest [19]. To minimize pump vibration, the internal flow variables of three impeller pumps have been examined using the computational fluid dynamics method. As per the program, the complex-impeller pump had such a considerable pressure difference, suggesting that its complex impeller can generate more excellent water. Using unstable time-frequency analysis, adding the splitter blade could substantially decrease the model pump's pressure-fluctuation amplitude. Two complicated impellers were also manufactured andthen used to compare the vibration response of the impellers with the previous and complicated impellers. As per simulation results, the complex impeller pump has a more incredible water head than the original pump. Meanwhile, the complex impeller benefits pump vibration frequency domain reduction, with vibration amplitudes reducing by 0.08 mm/s^2 at the blade approaching frequency [29]. In the last 50 years, turbo-machinery design has improved significantly. A turbo-machinery design is an interdisciplinary approach that includes stress, vibration, fluid dynamics, thermodynamics, and material selection analysis. Modal analysis is one of the most common and essential methods of analysis. Any mechanical component exposed to dynamic loading would be confined to dynamic loading analyses. The dynamic features of a centrifugal pump impeller were investigated in the work [20]. The natural frequencies and mode shapes were the only dynamic characteristics examined. A radial vanes impeller with a single entry was chosen for the research. The FEM was also used because it's been demonstrated to become a suitable replacement for an experimental method for assessing the vibrational behavior of a component or system. The impeller was modeled and simulated using the ANSYS Workbench tools respectively. Then the calculation of the Eigenvector and values is done. So, the results reveal that as the thickness of the impeller blades rose, so did the natural frequency of the impeller. The enhanced stiffness of the structure can be related to the rise in natural frequency [20].

Centrifugal pumps' impeller output width is essential for a variety of reasons. These consequences are explored in performance, pressure pulsations, vibrations generated by hydraulics, and noise levels, which are all discussed in the paper [21]. The volute's vibration and radiation of sound, when subjected to excitations of fluid force, were predicted using two techniques.

The complexity of today's industrial systems is increasing due to increased mechanization and automation. Any non-redundant machine component that fails impacts the entire system's operation. Many industrial types of machinery, such as pumps and motors, necessitate automated health monitoring and self-diagnosis (SDC) to boost availability and reliability. Failure is not prevented by condition monitoring; however, tracking specific machine parameters can anticipate the likelihood of future failure. Although various techniques for condition monitoring are available, the most effective methods for detecting flaws are vibration analysis, motor current signature analysis (MCSA), and irregularities in machine systems. The research [22] aims to create an SDC framework and use MCSA to inspect the impeller of a centrifugal pump. Different pump impeller states, such as average and defective impellers, are investigated in the time and frequency domains. There are significant differences, and a fault prediction strategy is suggested. As the severity of the impeller problem grows, so does the RMS, the vibration signal's value. T The vibration signal's peak value rises as the severity of the impeller fault increases, and the VPF can also be determined by visualizing the demodulated current spectrum [22]. Using the cyclic symmetry motion, stress analysis and Eigen pair determination of the typical turbocharger compressor impeller were tested. A simplified approach has also been tried to treat the hub and the blade as separate elements. The shortcomings of the simpler model have been exposed. The cyclic symmetric technique was used to analyze the findings of the finite element model [23]. The paper presents an effective method for analyzing nonlinear vibrations in centrifugal impellers that have been mistuned due to a crack. The primary goal is to look into the impact of vibration mistuning and crack characteristics of centrifugal impellers, as well as to look into crack detection systems that work. To begin and minimize the volume of input data needed for component mode synthesis, the whole design of an impeller is obtained with the help of a rotation transformation based on a sector model's finite element model (CMS). The damaged impeller is then a reduced-order model (ROM) generated using a CMS hybrid-interface approach. The crack surfaces' degrees of freedom are stored in the ROM to replicate crack breathing effects.

The Finite Element Method or experimental approaches commonly investigate problems with vibrating centrifugal pump impellers and other structures with complex geometry. The choice of mode shapes and natural frequencies is the initial stage in dynamic analysis. The motion of circular plate vibration can identify natural frequencies according to vibration mode shapes. The study [24] demonstrates how to classify the shapes of impeller vibration modes for a specific type of centrifugal pump and demonstrates that the impeller shown behaves similarly to a circular plate [24].

Centrifugal pump vibration was examined using critical pump speed, internal flow characteristics, and impeller force. Researchers conclude that raising the speed of the pump would not cause severe fluid vibration inside the pump. They used the ANSYS finite element analysis equations to determine the Rotor's system's natural frequency and critical speed. Authors realized that resonant frequency effects must end up causing the impeller to transient radial force-frequency inside an impeller which experiences transient radial force cyclical transition on a routine basis, with frequency size calculated by that of the product of the speed of impeller and number of blades The vibration signal's peak value rises as when the intensity of the impeller failure rises [25].

Monoblock centrifugal pumps can also be found in a diverse set of application areas. The Monoblock's centrifugal pump function is crucial in many applications, and condition monitoring is essential. Machine learning approaches to continuous vibration monitoring and analysis are gaining traction. For continuous monitoring and defect diagnostics, artificial neural networks and fuzzy logic were employed [26]. This study shows how to utilize the C4.5 decision tree technique to detect faults by analyzing quantitative data obtained from pleasant and unpleasant vibration data [26].

Centrifugal pumps are crucial components in many critical applications. Hence, their continuous availability is critical. The focus of this study is the concern of vibration-based fault diagnosis in centrifugal pumps. Many equipment problem detection and diagnostic approaches are used in a machine that vibrates status monitoring and fault detection. Numerous strategies to detect machinery defects use automatic signal classification to enhance the accuracy and remove defects affected by human subjective assessment. An adaptive network fuzzy inference system (ANFIS) was proposed in this work to determine the type of pump fault. Pump criteria to also be examined include healthy, cracked, and known to wear impellers, leakage, and cavitation. The FFT method is used to select these properties from vibration signals. The characteristics have been pumped through a dynamic neuro-fuzzy inference system as input variables. The system's efficiency has been confirmed by feeding the validation data set into the knowledgeable ANFIS model. The overall categorization accuracy was 90.67 percent, according to the results. This demonstrates that the system has a lot of promise for use in real-world applications as an intelligent problem diagnosis system [27]. Centrifugal compressors with fragile blades are becoming increasingly common as small gas turbines and turbochargers become more widely used in various technical fields. As a result, the impeller disc's outlet region has a smaller thickness. The impeller's delicate parts are incredibly vulnerable to blade vibrations, which can cause severe damage. This is done by comparing the radial-ending and backswept blades of two different impellers. The results show that coupling significantly impacts dynamic behavior and that impeller design is critical. The experimental results were found to be very consistent with the computational results [28].

The following fundamental dynamic equations can describe the disconnected masses of system 1 & system 2, respectively.

$$\ddot{x}_1 + \omega_1{}^2 x_1 - \frac{c_{1,2}}{M_1} x_2 = 0 \text{ with } \omega_1{}^2 = \frac{c_1 + c_{1,2}}{M_1} \tag{1}$$

$$\ddot{x}_2 + \omega_2{}^2 x_2 - \frac{c_{1,2}}{M_2} x_1 = 0 \text{ with } \omega_2{}^2 = \frac{c_2 + c_{1,2}}{M_2} \tag{2}$$

Analyzing a blade by itself or a disc or cover by itself is more straightforward than analyzing all three together. On the other hand, in practice, the impeller is a system that integrates the blade, the disc, and the cover (impeller with shroud). Compared to the dynamic behavior of a system consisting of just blades or discs, such a system's behavior becomes more complex. To rationalize fatigue failures and create a reliable impeller, it is essential to have a solid understanding of dynamic behavior. The finite element analysis (FEA) findings were performed on a straightforward impeller. These results help understand the behavior without adding to the complexity of the results, which paves the way for understanding the behavior of other similarly complex systems. In particular, it helps to rationalize the results of the system based on the results of the blade alone and the results of the disc alone. The outcomes of the FE analysis performed on an impeller, as well as a technique that assists in arriving at conclusionsregarding the possible resonance of an impeller [29]. Equation and free body diagram for a simple mass spring damper system are represented in Fig. 8.

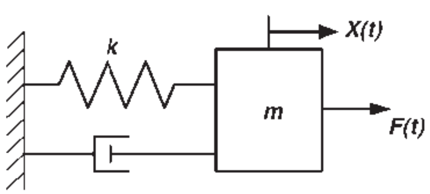

Figure 8. Single Spring-Mass-Damper System [29].

$$m.\,a + c.\,v + k.\,v = F(t).\cos(A) \tag{3}$$

This research presents a method for diagnosing problems in rotary machines using Machine Learning techniques. This research presents a support vector machine (SVM) algorithm as a potential solution for fault diagnosis of the rotational unbalance in the rotor. In recent years, support vector machines, also known as SVMs, have emerged as one of the most widely used classification approaches in the field of techniques for vibration analysis. Support vector machines are used in the process of classifying axis unbalanced faults. The experimental data were collected using a rotary machine model that consisted of a rigid-shaft rotor and flexible bearings. This particular experimental setup was designed to research vibration analysis. Several instances of faults involving unstable situations were successfully identified [30]. Impeller air and water frequency are given in Table 2, while the thrust force is given by the spring mass damper system equations as:

$$I\ddot{\theta} + c_t\dot{\theta} + k_t\theta = c_t\dot{\theta} =\acute{}\, -FR_o \tag{4}$$

$$m\ddot{q} + c_t\dot{q} + k_t q = c_t\dot{q}\,\acute{}= F \tag{5}$$

Table 2. Impellor air and water frequency.

Mode No.	f_0	f_w
1	249	188
2	270	204
3	324	245
4	378	286
5	768	581

A comparison between SKF6307 is given in Table 3, while the characteristics of impellors P-502B are reported in Table 4.

Table 3. Values of SKF6307.

Parameters	Values	Values
K	3.940×10^5	4.146×10^5
Diameter	57.5	65

Table 4. Characteristics of Impellor P-502B.

Parameters	Value
Material	GG25
Type	Closed
Equivalent thickness (m)	0.12
Diameter (m)	0.254-0.281-0.31
Density (kg/m^2)	7150
Mass (kg)	4.3-5.2-6
Polar moment of inertia (kg-m^2)	0.03467-0.05231-0.06153
Diametric moment of inertia (kg-m^2)	0.017338-0.02422-0.03283

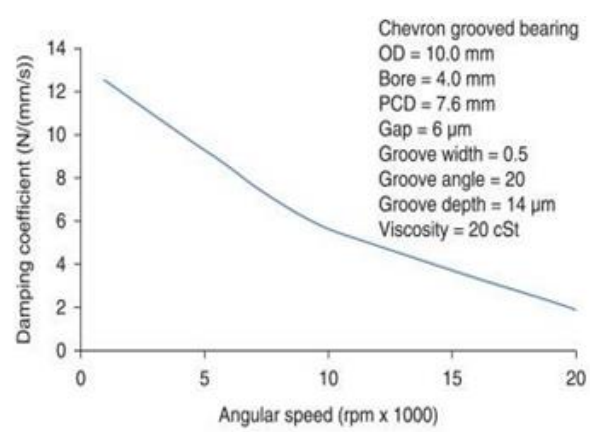

Figure 9. Angular speeds vs. damping coefficient [30].

Centrifugal compressors with skinny blades are becoming increasingly common as small gas turbines and turbochargers become more widely used in various technical fields. The impeller's delicate parts are incredibly vulnerable to blade vibrations, which can cause severe damage.

2. Mathematical Modelling

➢ ***Cavitation in a Centrifugal Pump Using Measurements of Vibrations and Flow Visualization***

The average RMS of the Segment at each second is calculated from the equations:

$$P_{WELCH}(\omega) = \frac{1}{5}\sum_{n=0}^{L-1} A[n]w[n]e^{-jwn} \quad (6)$$

$$P_{Band\ Limited} = \frac{1}{\omega}\int_{\omega_1}^{\omega_2} P_{WELCH}(\omega)d\omega \quad (7)$$

➢ ***Aerodynamically Induced Forces and Vibration Acting on Centrifugal Compressors***

Periodic External Forces are given as:

$$s(t) = \sum_1^{\infty} F_n cos(n\omega t + \theta_n) \quad (8)$$

$$x = \sum_1^{\infty} P_n cos(n\omega t + \theta_n - \emptyset_n) \quad (9)$$

$$P_n = \frac{D_n}{[(1-n^2\tau^2)^2 + (2\rho n\tau)^2]^2} \quad (10)$$

For arbitrary or non-periodic external forces:
f = the unit impulse force
F = the impulse force amplitude
$g(t)$ = response to the unit impulse forces

➢ ***Fourier Transform***

Fourier analysis transforms a signal f(t) from a time-based domain to a frequency-based one. The relationship is given as follows:

$$F(\omega) = \int_{-\infty}^{\infty} f(t)e^{-j\omega t}dt \quad (11)$$

$$x = \int_0^t f(\acute{t})g(t-\acute{t})d\acute{t} \quad (12)$$

➢ ***Dynamic Thrust Force***

There is an application of dynamic thrust force to the impeller blade.

$$C_1 = 0: F < \frac{2(\zeta_t\omega_t + 2\zeta\omega_n)}{(c_1 - c_0)a(\frac{1}{m} + \frac{R_o}{I})} \quad (13)$$

$$C_2 = 0: F < \frac{(\omega_n{}^2 + \omega_t{}^2 + 4\xi\omega_n\omega_t)}{(c_1 - c_0)a(2\omega_t\zeta_t\frac{1}{m} + 2\zeta_n\omega_n\frac{R_o}{I})} \quad (14)$$

$$C_3 = 0: F < \frac{2\xi\omega_t\omega_n{}^2 + 2\xi\omega_n\omega_t{}^2}{(c_1 - c_0)a(\frac{\omega_t{}^2}{m} + \omega_n{}^2\frac{R_o}{I})} \quad (15)$$

2.1. Significant Methodologies

Based on the literature review and by comparing the data, three shortlisted techniques are given below.

➢ ***Finite Element Analysis***

Finite element analyses, such as ANSYS, CREO, etc., are very significant in terms of the design and modeling of the impeller. FEM software's best if the following analysis is to be done:

✓ Flow field predictions of centrifugal Impeller
✓ Pump impeller's performance
✓ Flow leaking back (re-circulation) calculations
✓ Flow disturbances and Energy Transmission

➢ ***Blade Tip Timing and Strain Gauge (BTT)***

Mistuning issues in the pump are a significant problem. This problem can be solved using the blade tip timing and strain gauge method. It solves mistuning issues using an efficient reduced-order modeling method.

➢ ***Vibration Analysis and Motor Current Signature Analysis (MCSA)***

Vibration and motor current signature analysis (MCSA) can be used to solve the issue related to vibration analysis in centrifugal impellers. Vibration can cause the complete failure of the centrifugal impeller. Hence, their analysis is a crucial tool to determine the pump's good performance.

2.2. Limitations

The following are the limitations:

➢ There must be research on the aerodynamic excitation of rotor systems.

➢ Modeling the hub as bricks is three-dimensional to have an accurate impeller representation with an appropriate blade having various loading and boundary conditions. The blade comprises triangular shell elements, which can give more realistic results.

➢ There is an impact of different frequencies of impellor and also on the mode of different shapes of the system of rotors; totally floating bearings support them, as well as the impeller's gyroscopic effect on the rotor system as a whole would provide an improved comprehension of the problem.

➢ There must be reliable technology for crack detection in centrifugal impellers.

2.3. Summary of Findings

Results are being compared based on the method used, and the results are shown in Table 5.

Table 5. Summary of findings.

References	Approach	Results
Tilahun Nigussie 2015 [2]	ANSYS Turbo system–R 14.5	The design and analysis methodologies produce extremely accurate flow field predictions.
Shijo Shanmukhan 2016 [6]	CATIA V5	Structural analysis is used to determine the impeller's total deformation and strain energy as a result of the rotation.
Namdev T. Patil1 [7]	CFD	Numerical simulation is now recognized as an efficient method for solving fluid issues.
Da Costa, 2019 [30]	Support vector machines	Small sample sizes make the SVM a practical algorithm for machine learning.
Farah Elida , SEKAMAT [31]	ANSYS CFX	The impeller's efficiency will improve as the rotation speed is increased.
Y. Galerkin, A. Drozdov 2015 [5]	CFD calculations	For high-flow rate impellers, the representation of the absolute exit angle of flow along a trailing edge height is insufficient.
Mohamad Hazeri , 2015 [3]	CFD	CFD model can be adjusted to reduce the consumption of energy and reduce heat loss
Markus , 2019 [8]	CFD	Because of measurements for the Closed Impeller, a more oversized pump head is suggested than the Open Impeller,
T. Capurso 2019 [32]	ICEM CFD grid generator	Scaling the innovative geometry eventually revealed benefits in terms of power coefficient and space savings.
Amit Kumar, 2017 [9]	CFD and ANSYS	The pump impeller's performance is improved as the blade width at the impeller's exit increases.
Krishna Yadav, 2016 [33]	PTC CREO	The mixed flow pump's total efficiency rose by 5.81 percent at optimum levels.
LINDA, 2020 [34]	CFD	By lowering the quantity of flow that leaks back (recirculation) via the internal suction, pump efficiency at flow rates of 41.6 Kg/s was improved.
Krishna ,2015 [35]	PTC CREO	The pump's efficiency is 83 percent for an initial input angle of 20.080 and an exit angle of 16.280
James M. Strokes, 2018 [10]	CFD	Flow disturbances that can induce forced vibration include stalling impellers, stalling diffusers.
Shijie GUO , 2004 [12]	NASTRAN	Resonance can also be induced when the impeller's inherent frequency corresponds with the sideband frequencies.
Hui Sun, 2018 [13]	Fast Fourier transform (FFT)	The recognition of various types of flaws may provide vital evidence to detect faults while the pump is running.
Georgios [14]	Computational fluid dynamics (CFD)	A decrease in value causes a growth in the number of bubbles, which increases the noise and vibration produced by the machine.
Mehran Jahangiri, 2018 [15]-[16]	Vibration analysis (FFT).	A clogged impeller hindered the fluid transfer, and the flow rate dropped compared to a normal impeller, the electrical power consumption decreased accordingly.
Zhao, Xinwei, 2021[28]	Blade tip timing and strain gauge (BTT)	It helps to solve mistuning issues using an efficient reduced-order modeling method.
Waleed Abdulkarem, 2014 [17]	Crack fault diagnosis (power spectrum)	The fundamental Frequency (impeller frequency) increases as the impeller fracture size increases
Irfan, Muhammad, 2019 [18]	Electric diagnostics technology	Pump failure results in significant production losses, so the creation of a cost-effective and user-friendly condition monitoring system is critical.
Algebraic, A. , 2012 [36]	Experimental Setup (YD3 8131 Model)	This study is used to extract various critical aspects that represent the excellent condition of the pump, pump operation as well as pump energy consumption.
Shooshtari, Alireza, 2021 [37]	Timoshenko theory	An impeller can increase vibration amplitude by up to 52%.
Al-Obaidi, A. R., 2019 [38]	Temporal domain analysis (TDA) and Fast Fourier Transform (FFT)	Values for mean and RMS vibratory amplification can help anticipate cavitation in centrifugal pumps.
Rusiński, E., 2014 [19]	Fourier analysis	Vibrations measured in the casing in both steady and unstable states have the potential to produce damage such as construction fractures.
Yuan, Ye , 2019 [39]	Computational fluid dynamics	The complicated impeller pump has a higher water head than the original pump.
Karuppanan, S., 2014 [20]	ANSYS Bladegen and ANSYS Workbench	The thickness of the impeller disc had a substantial impact on the impeller's inherent frequency.
Liu, Houlin, 2014 [21]	Combined CFD/FEM structural vibration study	The effects of centrifugal pumps' sound pressure on the structure appear to be minor.
Qian, Bo, 2020 [40]	CFD	When distribution of blade thickness changes, energy transmission in impeller is also reallocated
V. RAMAMURTI., 1994 [23]	Stress analysis and Eigen pair	The cyclic symmetric technique was used to analyze the findings of the finite element model.
Wang, Shuai, 2014 [41]	CMS hybrid-interface	The change and division of two different resonance frequencies with exactly equal nodal diameters are perhaps the most measurable influences of mistuning and cracks on vibration response.
Zhao, X. Zhou, Q., 2019 [42]	Flow channel stall cell evolution	Blade vibration is monitored using tip timing sensors and strain gauges.
Oza, M. N. ,Shah 2020 [43]	CERO and ANSYS	Both methods in terms of natural frequencies have been evaluated by comparing, and the outcomes were observed to be in satisfactory correlation, indicating that the FE model is genuine
Samir Lemeš, 2002 [24]	ANSYS	The motion of circular plate vibration can be used to identify natural frequencies
Zhao, W. Y., 2013 [25]	Fluent (ANSYS)	To overcome the effect of resonance, the frequency range should be less than resonance in the case of transient radial force-frequency
Sakthivel, N. R. , 2010 [26]	Machine learning	This study shows how to utilize the C4.5 decision tree technique to diagnose faults using statistical features taken from excellent and bad vibration data
Saeid Farokhzad, 2013 [27]	The FFT technique	The overall categorization accuracy was 90.67 percent.
Dirk Hagelstein, 1998 [28]	FE code computations	Computational and experimental results matched well.
Murari P. Singh , 2003 [29],	FEA Analysis	These results help understand behavior without complexity, paving the way to understanding similar complex systems.
Da Costa, 2019 [30]	Support vector machines	Small sample sizes make the SVM a practical algorithm for machine learning.
Han, Hyungsuk, 2020 [44]	FEM Analysis	Increasing dynamic flow causes self-excited blade vibration. - FEM analysis estimates induced force reduces maximum stress by 37.6%.

2.4. Method to Remove Vibration in Centrifugal Pump

The following are the methods and their solution for control of vibration in impeller Pump Cavitation: Cavitation takes place when the pump's positive suction head is insufficient. When the liquid pressure at the inlet of the impeller is equivalent to the liquid-vapor pressure, air pockets form and collapse. The sound of these air pockets popping can easily be identified as pump cavitation. It sounds like rocks inside the pump are rumbling, or you can hear distinct air-popping sounds. Aside from the noise, pump cavitation is marked by a higher energy need for the pump to work than usual. Method to prevent Cavitation: The following are the methods through which cavitation can be prevented. Make sure the pump's filters and strainers are in good working order. Check the filters and strainers of the pump for proper operation. If the pump curve is not ideal, reconsider the pump design. Bent Pump Shaft: High axial vibrations are caused when the pump shaft is bent. Bending pump shafts usually occur near the coupling joints. Method to Bent Pump Shaft: Dial indicators can be used to prevent the bent pump shaft and also the vibration that is the result of that bent pump shaft. Pulsation occurs when a pump continues to operate near the shut-off head. The following factors cause pump flow pulsation: Valves that leak, improper spring rates, improper feed, using several pumps on a single header, piping systems with flow restrictions. We can avoid pulsation by using a suction stabilizer, which keeps the displaced fluid in contact with the plunger at all times. Pump Impeller Imbalance in Fig. 10. Vibrations and heat production are caused whenever there is an imbalance in the pump assembly. When the pump's impellers are correctly balanced, the bearings last longer, decreasing the number of vibrations produced by the pump. Some of the risks associated with an imbalanced pump impeller include the following: Failure of the bearings, failure of pump seals, inappropriately high vibrations, and deflected shafts are the result in deflection and seizures related to the pumps.

Figure 10. Impeller Imbalance.

Method to reduce vibration due to Impeller Imbalance: A pump maintenance engineer will help you overcome these issues by precision aligning the impellers. Bearing Failure: Failure of the bearings in the pump is one of the primary causes of vibrations. Although your pump could run trouble-free for 20,000 hours, the bearings inside of it will fail well before that point. Failure of pump bearings can be caused by a wide variety of factors, including but not limited to corrosion, inadequate lubrication; contamination, excessive wear, and tear; extreme temperatures, and overheating. In addition to these problems, the incorrect selection of bearings is another primary factor contributing to pump bearing failure. Method to reduce vibration due to Bearing Failure: We can solve the problems with the pump bearings if we lubricate them regularly using the oils that the pump manufacturer recommends. Additionally, bearings should be replaced regularly to prevent excessive vibrations. Shaft Misalignment: Misalignment of the shaft can also result in excessive vibrations, similar to how an impeller imbalance can. Misalignments of the shaft in Fig. 11 are difficult, if not impossible, to detect from the outside and require the assistance of a trained professional. If vibrations persist even after the conditions above have been corrected, the problem may be caused by a shaft not appropriately aligned. The following symptoms may indicate that your pump's shaft is not aligned correctly: An excessive amount of oil leaks, in addition to the bearing seals. Failures in the couplings. Foundation bolts or couplings that are too loose. Excessive oil discharges.

Figure 11. Shaft misalignment.

3. Proposed Methodology

3.1. Different Sceneries for Vibration in Centrifugal Impeller

The proposed methodology for the centrifugal impellor vibrational problem related to the impeller is given in the Flow chart is shown in Fig. 12.

The forces used for this method are as follows

- ***Free Vibration***

System Response is studied without the implementation of Force

- ***Step Input***

Step input is used to calculate the system response

- ***Harmonic Force***

Defects in the pumps, such as misalignment, unbalance is captured as a harmonic force.

Values used for modeling of centrifugal impeller are represented in Table 6.

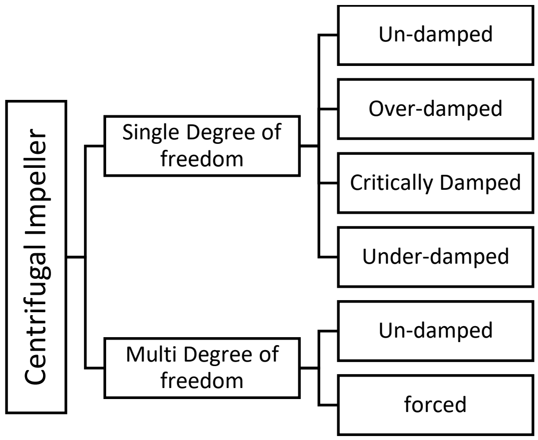

Figure 12. Proposed flow chart for analysis.

Table 6. Values used in calculation.

Sr#	Parameter	Symbol	Value
1	Frequency	ω	150 rad/s
2	Mass of pump	M1	100 kg
3	Mass of foundation	M2	1000 kg
4	Stiffness of impeller	K1	5x10e5 N/m
5	Stiffness of foundation	K2	2x10e7 N/m
6	Rotating imbalance	me	0.1 kg
7	Damping of pump	C1	10 Ns/m
8	Damping of foundation	C2	100 Ns/m

3.2. Implementation

➢ ***Free Vibration (Undamped System)***

Free vibration, as in Fig. 13 occurs when no vibration force is being applied from the outside. In most cases, the solution to a free vibration will approximate a sinusoidal pattern. There is no question that vibrations can occur across the entire spectrum of frequencies. There will typically be at least one frequency with growing amplitude, and in some cases, there may be more than one. A free vibration will have a constant amplitude up to the edge of its stability. Itneither expands nor contracts over time.

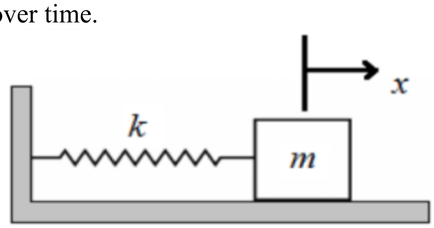

Figure 13. Free vibration un-damped system.

The equations of free vibration un-damped system are given by:

$$m\ddot{x} + kx = 0 \tag{16}$$

$$x = x_o \cos(\omega_n t) + \frac{\dot{x}_o}{\omega_n} \sin(\omega_n t) \tag{17}$$

where m is the mass of the impeller and k is the stiffness of the impeller. The natural frequency of the impeller is given by:

$$\omega_n = \sqrt{\frac{k}{m}} \tag{18}$$

- ***Free Vibration (damped System)***

Adding a "vicious" damper to the impeller model results in the generation of a force proportional to the speed at which the mass is moving. The proportionality constant c is also known as the damping coefficient, and its units are force multiplied by velocity. The equation is given by

$$m\ddot{x} + c\dot{x} + kx = 0 \tag{19}$$

where m is the mass of the impeller, c is the damping constant, and kis the stiffness of the impeller.

- ***Under damped***

The term "un-damped" refers to the absence of any energy loss associated with motion (whether intentional, by adding dampers, or unintentional, through drag or friction). Without the application of any additional forces, an un-damped system will continue to vibrate forever. When a system is under-damped, it oscillates slightly before returning to its normal state when you give it a nudge (also known as an "impulse").

$$x(t) = Xe^{-\zeta\omega_n t}\cos\left(\sqrt{1-\zeta^2}\,\omega_n t - \phi\right) \tag{20}$$

$$X = \frac{\sqrt{{x_o}^2{\omega_n}^2 + {\dot{x}_o}^2 + 2\zeta\omega_n x_o \dot{x}_o}}{\sqrt{1-\zeta^2}\,\omega_n} \tag{21}$$

$$\phi = \tan^{-1}\left(\frac{\dot{x}_o + \zeta\omega_n x_o}{x_o\sqrt{1-\zeta^2}\,\omega_n}\right) \tag{22}$$

The damped frequency of the impeller is given by:

$$\omega_d = \sqrt{1-\zeta^2}\,\omega_n \tag{23}$$

- ***Damping constant***

A ratio known as the damping ratio (also known as the damping factor and percent critical damping) is used to characterize the amount of damping in a system. Other names for this ratio include the following: This damping ratio is simply the actual damping divided by the minimum amount of damping necessary to reach the critical damping.

$$\zeta = \frac{c}{c\sqrt{km}} \tag{24}$$

- ***Critically Damped***

When a system is said to be critically damped, it means that when you give it a nudge (also known as an "impulse"), it willreturn to its rest state in the shortest possible time without oscillating.

$$c = c_C \tag{25}$$

$$(t) = (c_1 + c_2 t)^{-\omega_n t} \tag{26}$$

- ***Over Damped***

If a system is over-damped, it responds to a push (also known asan "impulse") by taking its time and returning to its resting statemuch more slowly than is strictly required.

$$x(t) = c_1 e^{(-\zeta+\sqrt{\zeta^2-1})\omega_n t} + c_2 e^{(-\zeta-\sqrt{\zeta^2-1})\omega_n t} \tag{27}$$

- ***Forced Vibration***

When a time-varying disturbance (load, displacement, velocity, or acceleration) is applied to a mechanical system, this results in the phenomenon known as forced vibration. The disturbancemay come from an input that is periodic and in a steady state, an input that is transient, or a random input. There is a possibility that the periodic input will be a disturbance that is not harmonic. The mass Spring damper system of the impeller and the steady state are given as:

$$m\ddot{x}+c\dot{x}+kx=F \tag{28}$$

$$x_p = \frac{F_o}{k} \tag{29}$$

- ***Damped Harmonic Vibration***

Vibrating systems known as damped harmonic oscillators gradually reduce the amplitude of their vibrations for their operation. Because nearly all physical systems involve factors like air resistance, friction, and intermolecular forces, which cause energy to be lost in the system as heat or sound, realistic oscillatory systems must consider damping. The equation for spring-mass damper under the harmonic force of impeller is given by

$$m\ddot{x} + c\dot{x} + kx = F_o \cos\omega t \tag{30}$$

where Fo is the force on the impeller:

$$X = \frac{F_o}{\sqrt{(k - mw^2)^2 + (c\omega)^2}} \tag{31}$$

$$\phi = \tan^{-1}\left(\frac{c\omega}{k - mw^2}\right) \tag{32}$$

$$x_p = X\cos(\omega t - \phi) \tag{33}$$

$$x_n = X_o\, e^{-\zeta\omega_n t}\cos(\omega_d t - \phi_o) \tag{34}$$

$$X_o = \frac{\sqrt{x_o{}^2\omega_n{}^2 + \dot{x}_o{}^2 + 2\zeta\omega_n x_o\dot{x}_o}}{\sqrt{1-\zeta^2}\,\omega_n} \tag{35}$$

$$\phi = \tan^{-1}\left(\frac{\dot{x}_o + \zeta\omega_n x_o}{x_o\sqrt{1-\zeta^2}\,\omega_n}\right) \tag{36}$$

$$x(t) = x_n(t) + x_p(t) \tag{37}$$

➢ ***Two Degree of Freedom System***

A system is considered to have two degrees of freedom, as represented in Fig. 14. if its equation of motion can only be wholly described using two coordinates. When the coordinates in question can be understood independently, we refer to them as generalized coordinates.

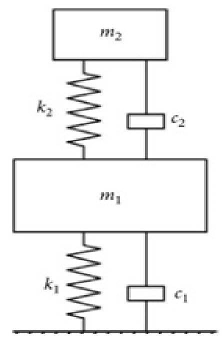

Figure 14. Proposed flow chart for analysis.

There are two equations to solve for a system with two degrees of freedom, one for each mass in the system (precisely one for each degree of freedom). In most cases, they take the shape of coupled differential equations; this means that every equation in the system involves all of the coordinates. If it is assumed that each coordinate has a harmonic solution, then the equations of motion will lead to a frequency equation, which will give you two natural frequencies for the system.

Mass 2(Mass of Shaft)

$$m_1\ddot{x}_1 + (c_1 + c_2)\dot{x}_1 - c_2\dot{x}_2 + (k_1 + k_2)x_1 - k_2x_2 = 0 \tag{38}$$

$$\begin{bmatrix} m_1 & 0 \\ 0 & m_2 \end{bmatrix}\begin{Bmatrix} \ddot{x}_1 \\ \ddot{x}_2 \end{Bmatrix} + \begin{bmatrix} c_1 + c_2 & -c_2 \\ -c_2 & c_2 \end{bmatrix}\begin{Bmatrix} \dot{x}_1 \\ \dot{x}_2 \end{Bmatrix} + \begin{bmatrix} k_1 + k_2 & -k_2 \\ -k_2 & k_2 \end{bmatrix}\begin{Bmatrix} x_1 \\ x_2 \end{Bmatrix} = \begin{bmatrix} 0 \\ 0 \end{bmatrix} \tag{39}$$

If c_1 and c_2 = 0 then

$$\begin{bmatrix} m_1 & 0 \\ 0 & m_2 \end{bmatrix}\begin{Bmatrix} \ddot{x}_1 \\ \ddot{x}_2 \end{Bmatrix} + \begin{bmatrix} k_1 + k_2 & -k_2 \\ -k_2 & k_2 \end{bmatrix} = \begin{bmatrix} 0 \\ 0 \end{bmatrix} \tag{40}$$

$$det\begin{bmatrix} -m_1\omega^2 + k_1 + k_2 & -k_2 \\ -k_2 & -m_2\omega^2 + k_2 \end{bmatrix} = 0 \tag{41}$$

$$r_1 = \frac{X_2^{(1)}}{X_1^{(1)}} = \frac{-m_1\omega_1^2 + k_1 + k_2}{-k_2} \quad (42)$$

$$r_2 = \frac{X_2^{(2)}}{X_1^{(2)}} = \frac{-m_1\omega_2^2 + k_1 + k_2}{-k_2} \quad (43)$$

For Mass2

$$m_2\ddot{x}_2 - c_2\ddot{x}_1 + c_2\dot{x}_2 - k_2x_1 + k_2x_2 = 0 \quad (44)$$

For Mass 1

$$m_1\ddot{x}_1 + (c_1 + c_2)\dot{x}_1 - c_2\dot{x}_2 + (k_1 + k_2)x_1 - k_2x_2 = 0 \quad (45)$$

$$\begin{bmatrix} m_1 & 0 \\ 0 & m_2 \end{bmatrix}\begin{Bmatrix} \ddot{x}_1 \\ \ddot{x}_2 \end{Bmatrix} + \begin{bmatrix} c_1 + c_2 & -c_2 \\ -c_2 & c_2 \end{bmatrix}\begin{Bmatrix} \dot{x}_1 \\ \dot{x}_2 \end{Bmatrix} + \begin{bmatrix} k_1 + k_2 & -k_2 \\ -k_2 & k_2 \end{bmatrix}\begin{Bmatrix} x_1 \\ x_2 \end{Bmatrix} = \begin{bmatrix} 0 \\ 0 \end{bmatrix} \quad (46)$$

$$\begin{bmatrix} m_1 & 0 \\ 0 & m_2 \end{bmatrix}\begin{Bmatrix} \ddot{x}_1 \\ \ddot{x}_2 \end{Bmatrix} + \begin{bmatrix} k_1 + k_2 & -k_2 \\ -k_2 & k_2 \end{bmatrix} = \begin{bmatrix} 0 \\ 0 \end{bmatrix} \quad (47)$$

$$det\begin{bmatrix} -m_1\omega^2 + k_1 + k_2 & -k_2 \\ -k_2 & -m_2\omega^2 + k_2 \end{bmatrix} = 0 \quad (48)$$

$$\omega_1^2, \omega_2^2 = \frac{1}{2}\left\{\frac{(k_1 + k_2)m_2 + k_2m_1}{m_1m_2}\right\} \mp \frac{1}{2}\sqrt{\left(\frac{(k_1 + k_2)m_2 + k_2m_1}{m_1m_2}\right)^2 - 4\left(\frac{(k_1 + k_2)k_2 - k_2}{m_1m_2}\right)} \quad (49)$$

$$r_1 = \frac{X_2^{(1)}}{X_1^{(1)}} = \frac{-m_1\omega_1^2 + k_1 + k_2}{-k_2} \quad (50)$$

$$r_2 = \frac{X_2^{(2)}}{X_1^{(2)}} = \frac{-m_1\omega_2^2 + k_1 + k_2}{-k_2} \quad (51)$$

Modes of Vibration

$$\vec{X} = \begin{Bmatrix} X_1^{(1)} \\ X_2^{(1)} \end{Bmatrix} = \begin{Bmatrix} X_1^{(1)} \\ r_1X_2^{(1)} \end{Bmatrix} \quad (52)$$

$$\vec{X} = \begin{Bmatrix} X_1^{(2)} \\ X_2^{(2)} \end{Bmatrix} = \begin{Bmatrix} X_1^{(2)} \\ r_2X_1^{(2)} \end{Bmatrix} \quad (53)$$

where

$$X_1^{(1)}(t) = X_1^{(1)}\cos(\omega_1 + \emptyset_1)$$
$$X_1^{(2)}(t) = X_1^{(2)}\cos(\omega_2 + \emptyset_2)$$

where

$$X_1^{(1)} = \frac{1}{r_2 - r_1}\left[\sqrt{(r_2x_{10} - x_{20})^2 + \frac{(-r_2\dot{x_{10}} \dot{-} \dot{x_{20}})^2}{\omega_1^2}}\right]$$

$$X_1^{(2)} = \frac{1}{r_2 - r_1}\left[\sqrt{(r_1x_{10} - x_{20})^2 + \frac{(-r_1\dot{x_{10}} \dot{-} \dot{x_{20}})^2}{\omega_2^2}}\right]$$

$$\emptyset_1 = \tan^{-1}\left\{\frac{-r_2\dot{x_{10}} \dot{+} \dot{x_{20}}}{\omega_1(r_2x_{1(0)} - x_{20})}\right\} \quad (54)$$

$$\emptyset_2 = \tan^{-1}\left\{\frac{-r_1\dot{x_{10}} \dot{+} \dot{x_{20}}}{\omega_2(-r_1x_{1(0)} - x_{20})}\right\} \quad (55)$$

- ***Free Vibration Response of 2DOF (Undamped)***

$$x_1(t) = X_1^{(1)}(t) + X_1^{(2)}(t) = X_1^{(1)}\cos(\omega_1(t) + \emptyset_1) + X_1^{(2)}\cos(\omega_2 + \emptyset_2) \quad (56)$$

$$x_2(t) = X_2^{(2)}(t) + X_2^{(1)}(t) = r_1X_1^{(1)}(t) + r_2X_1^{(2)}(t) \quad (57)$$

$$x_2(t) = r_1(X_1^{(1)}\cos(\omega_1(t) + \emptyset_1)) + r_2X_1^{(2)}\cos(\omega_2 + \emptyset_2)) \quad (58)$$

- ***Time Constant (T_c)***

It is defined as time constant. At this time, natural response e^{-st} decays to 37% of its original values and step response rises to 63% of final value.

$$T_c = \frac{1}{a} \quad (59)$$

- ***Rise Time (T_r)***

It is defined as the time it takes for the system response to go from 10% to 90% of its final value.

$$T_s = \frac{4}{a} \quad (60)$$

- ***Characteristics of 2nd order Response***

Time to reach 1st peak.

$$T_p = \frac{\pi}{\omega_n\sqrt{1 - \zeta^2}} \quad (61)$$

- ***Percentage Overshoot***

The amount is expressed as a percentage by which a response overshoots beyond the final value at a steady state in the first peak.

$$\%OS = e^{-(\frac{-\xi\pi}{\sqrt{1-\zeta^2}}} x100 \tag{62}$$

- ***Settling Time***

The amount of time required for the response to reach and maintain a value within +2% of the steady-state value. This is provided by:

$$T_s = \frac{4}{\zeta\omega_n} \tag{63}$$

3.3. Magnification Factor and Transmissibility

- ***Deformation Response Factor or Magnification Factor***

Displacement of a Mass-Spring-Damper (MSD) system, a free-body diagram is shown in Fig. 15, also known as the vibratory response of a system when it is subjected to a harmonic load about some different frequency ratios $(\frac{\omega}{\omega_n})$ are being discussed here.

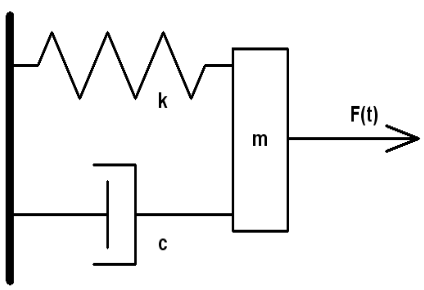

Figure 15. Mass-Spring-Damper systems under harmonic load.

where f(t) is equal to $F_o Sin(\omega t)$. The following equation gives the MSD system response to harmonic load:

$$u(t) = \frac{\frac{F_o \sin(\omega t - \emptyset)}{k}}{\sqrt{(1-(\frac{\omega}{\omega_n})^2)^2 + (2\zeta\frac{\omega}{\omega_n})^2}} \tag{64}$$

Since an MSD system's transient response decreases exponentially with time, its contribution to the total response (transient + steady-state) is negligible.

$$(t) = \frac{F_o}{k} * MF \tag{65}$$

where the MF is given by:

$$MF = \frac{1}{\sqrt{(1-(\frac{\omega}{\omega_n})^2)^2 + (2\zeta\frac{\omega}{\omega_n})^2}} \tag{66}$$

The system response is given in Fig. 16.

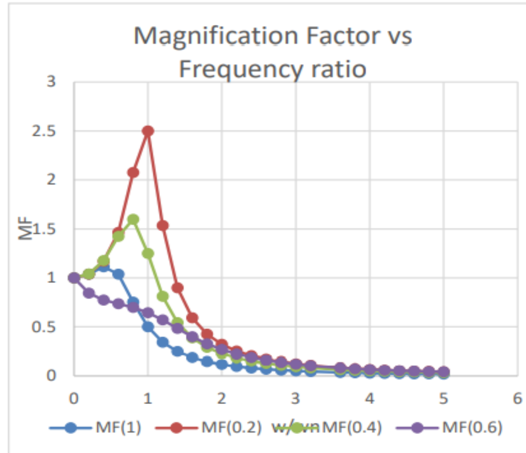

Figure 16. Magnification Factor vs. Frequency ratio

where MF (1) represents the value of MF at a value of ζ = 1 and so on. The effect of these will be discussed later in the results sections.

At ω/ω_n = 0, MF = 1. This indicates that the system or machinery will have static deflection when it is in a stationary condition. (That is to say, the response of a system takes the form of a sine wave, and its maximum amplitude is f_o/k. When there is a greater amount of damping, there is a decrease in the peak amplitude of the vibration. In addition, there is a shift to the left in the peak value for the system's displacement response. This is because heavy machines have a low natural frequency. The conclusion from the Transmissibility ratio follows. At ω/ω_n = 0, TR will be equal to 1.

- ***Transmissibility***

For example, a centrifugal pump sitting on the base (steel base frame). Let us suppose that there is a flaw in the pump (such as an imbalance in the impeller, a misalignment, a shaft that has been bent, etc.) and that this flaw caused the generation of harmonic load, which in turn caused the pump to vibrate as shown in Fig. 17.

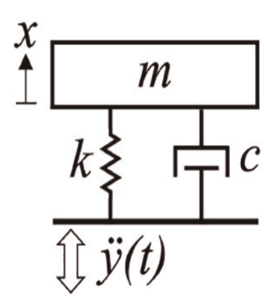

Figure 17. Spring mass damper model of a centrifugal pump and its base.

The amount of force transferred to the pump base due to the vibrations produced by the pump is something that interests us. The transmissibility ratio, also known as TR, is the ratio of the maximum transmitted force to the applied force.

$$TR = \frac{F_T}{F_0} = \sqrt{\frac{1 + (2\zeta\frac{\omega}{\omega_n})^2}{\sqrt{(1 - (\frac{\omega}{\omega_n})^2)^2 + (2\zeta\frac{\omega}{\omega_n})^2}}} \quad (67)$$

With the help of this equation, a graph will be generated, as shown in Fig. 18.

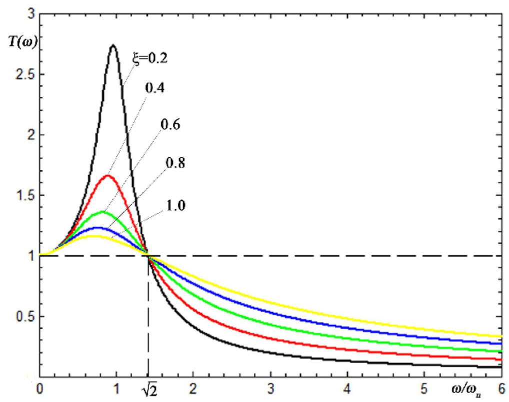

Figure 18. Transmissibility ratio vs. frequency ratio.

At ω/ω_n = 0, MF = 1. This indicates that the system or machinery will have static deflection when it is in a stationary condition. (That is to say, the response of a system takes the form of a sine wave, and its maximum amplitude is f_o/k. When there is a greater amount of damping, there is a decrease in the peak amplitude of the vibration. In addition, there is a shift to the left in the peak value for the system's displacement response. This is because heavy machines have a low natural frequency. The conclusion from the Transmissibility ratio follows. At ω/ω_n =0, TR will be equal to 1.

4. Results

The outcomes of the system under different applied forces are discussed in this section. A graph is plotted using MATLAB.

4.1. Free Vibration

➢ ***Response plot of un-damped Single DOF for mass-spring system***

The graph in Fig. 19 gives a response of un-damped SDOF of the mass spring system of the impeller

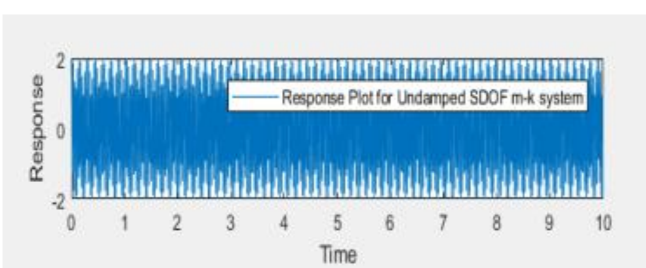

Figure 19. Un-damped SDOF of the mass-spring system showing the amplitude of the displacement does not decrease over time.

Fig. 19 shows that because there is no mechanism for reducing the amount of energy/Force contained inside the system over time, the amplitude of the displacement does not decrease over time.

➢ ***Response plot of under-damped Single DOF for a mass-spring damper system***

The following graph gives a response of under-damped SDOF of the mass-spring damper system of the impeller.

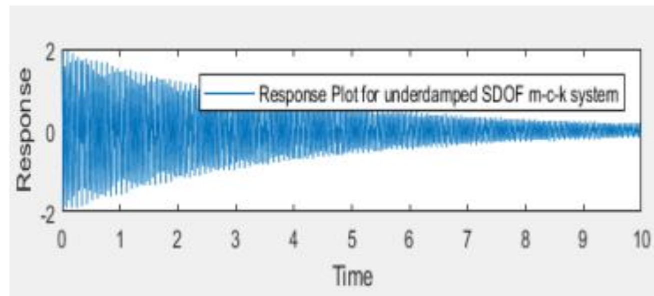

Figure 20. Under-damped SDOF of the mass-spring damper system showing amplitude of the displacement decreases.

Fig. 20 shows that the amplitude of the displacement decreases in an exponential manner. The period and frequency of a system with a small amount of damping are almost identical to those of simple harmonic motion, but the amplitude gradually decreases. This occurs due to the non-conservative damping force's removal of energy from the system, which typically takes the form of thermal energy.

➢ ***Response plot of critically damped Single DOF for a mass-spring damper system***

The following graph gives the response of critically damped SDOF of the mass-spring damper system of the impeller.

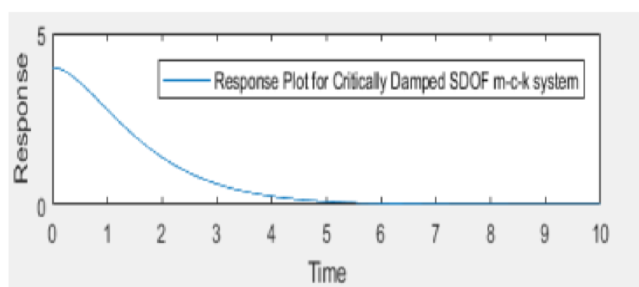

Figure 21. Critically damped Single DOF for a mass-spring-damper system.

Fig. 21 shows that a damped oscillator can get closer to zero amplitude through critical damping than any other method. If insufficient damping, the system will reach the zero position more quickly, oscillating around it. The approach to zero is slowed down when there is an excessive amount of damping (over-damping). The point at which the damping coefficient is equal to the un-damped resonant frequency of the oscillator is known as the critical damping point.

- ***Response plot of Overdamped damped Single DOF for a mass-spring-damper system***

Response of over-damped SDOF of a mass-spring-damper system of the impeller is given as:

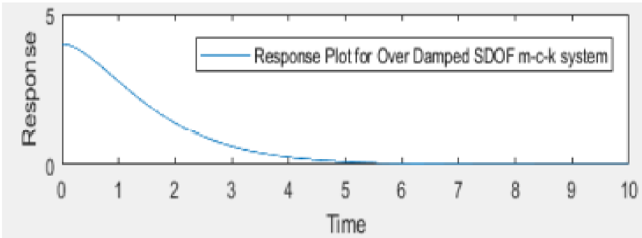

Figure 22. Overdamped damped single DOF for a mass-spring-damper system

Fig. 22 shows if an oscillator is over-damped, its approach to a state of zero amplitude will be slower than in the case of critical damping, where the level of damping is just right. There is a positive relationship between the damping coefficient and the un-damped resonant frequency.

4.2. Forced Vibration

- ***Response plot of un-damped Single DOF for a mass-spring system with step input***

Response of un-damped SDOF of the mass-spring system of an impeller with step input is given as:

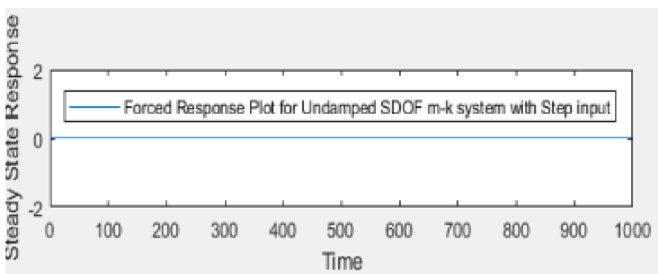

Figure 23. Step input for undamped SDOF system.

The responses in Fig. 23 make it abundantly clear that the fact that the applied loading was done transiently can have a sizeable impact on the obtained response.

- ***Response plot of un-damped Single DOF for a mass-spring system with Harmonic Force***

Response of un-damped SDOF of a mass-spring system of the impeller with Harmonic Force is given as:

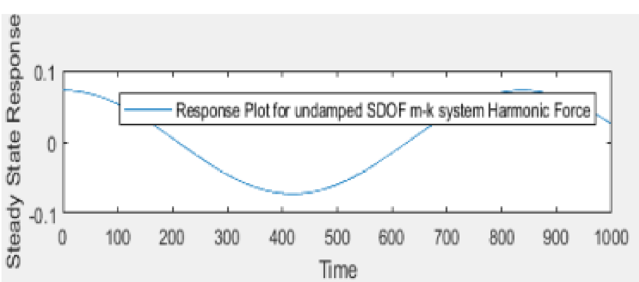

Figure 24. Un-damped single DOF for mass system with harmonic force.

Fig. 24 shows that there will be repeated harmonic motion, and no damping will stop the motion of that harmonic force.

- ***Response plot of damped Single DOF for a mass-spring system with Harmonic Force***

Response of damped SDOF of the mass-spring system of the impeller with Harmonic Force is given in Figs. 25 and 26.

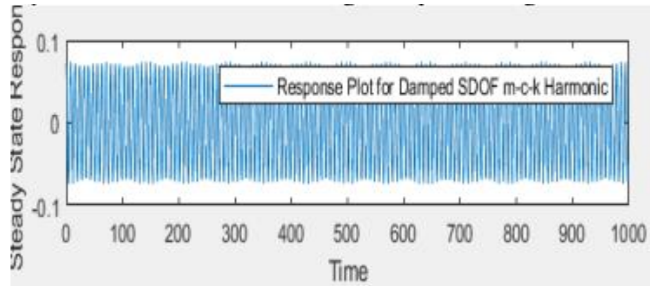

Figure 25. Damped harmonic.

The term "damped simple harmonic motion" refers to these periodic motions with progressively decreasing amplitude.

- ***Results of Transient Response of un-damped 2DOF System***

Transient response of un-damped 2DOF of the mass-spring system of the impeller is as:

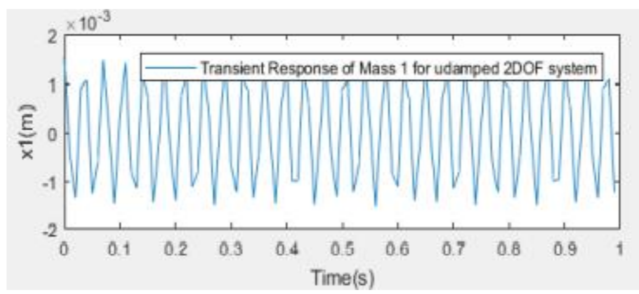

Figure 26. For the mass of impeller.

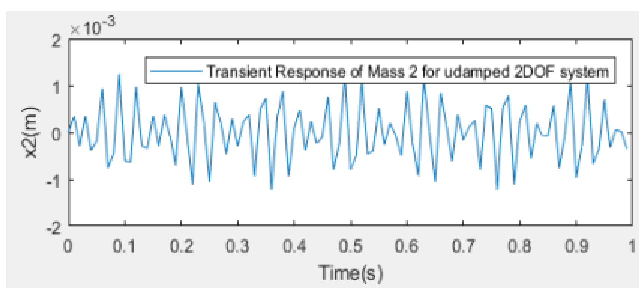

Figure 27. For a mass of the shaft.

Fig. 27 shows that according to this graph, the general vibration of the system is made up of the aggregate of all of the system's different vibration modes (which all vibrate at their discrete frequencies). By starting the system with a variety of different initial conditions, we can control the magnitude of the contribution made by each mode.

➢ ***Calculated Values of Constants***

Depending upon the values we have calculated for the impeller, we found the following values, which are represented in Table 7.

Table 7. Calculated values of constants.

T_p	%OS	T_s	T_c	T_r
0.01403	99.923	79.86	1.056	3.79

➢ ***Results of Deformation Response Factor***

- When $\frac{\omega}{\omega_n}$ <1 then the force excitation period is more extended than the system's natural frequency, and it refers to the lower frequency ratio so:

$$u(t) = \frac{F_o}{k} \tag{68}$$

The following things can be observed from this:

✓ Damping does not affect a system's vibratory response.
✓ The stiffness of a system is what determines its vibratory response.

- When $\frac{\omega}{\omega_n}$ =1, then harmonic force equals the system's natural frequency, so the final equation becomes:

$$u(t) = \frac{F_o}{2\zeta k} \tag{69}$$

✓ Damping is responsible for controlling the vibratory response of a system.
✓ When a machine's damping is zero, its vibration amplitude at its natural frequency will be infinite, resulting in the machine failing catastrophically.

- When $\frac{\omega}{\omega_n}$ >1, then, when compared to the system's natural frequency, the time of the force's excitation is significantly shorter. Equation becomes:

$$u(t) = \frac{F_o}{m\omega^2} \tag{70}$$

So it represents
✓ The mass of a system determines its resonant frequency and thus controls the vibratory response of the system.
✓ The damping of a system does not affect the vibratory response of the system.

5. Conclusion

It is concluded that the vibrational analysis of the centrifugal impellors can be done using the finite element method, which is the good and precise method. Other methods that include vibrational studies related to impellors are Blade tip timing and strain gauge (BTT), vibration analysis, and motor current signature analysis (MCSA). The conclusion from Single Degree of freedom Damped harmonic oscillators is characterized by non-conservative forces, which cause the oscillators' energy to be lost. Damping at the critical level brings the system back to equilibrium as quickly as possible while preventing it from overshooting. A system with insufficient damping will oscillate between the two positions of equilibrium. Compared to a critically damped system, an over-damped system moves toward equilibrium at a much more decreasing rate.

6. Recommendations

The likelihood of cavitation induced by the pump in response to vapor formation in the fluid region and impeller is a new area of research topic in which work needs to be done. Pulsation occurs when a pump continues to operate near the shut-off head, and high axial vibrations are caused when the pump shaft is bent. Bending pump shafts usually occur near the coupling joints. These are also new areas for research.

References

[1] A. Engeda, "Early historical development of the centrifugal impeller," in Turbo Expo: Power for Land, Sea, and Air, 1998, p. V005T16A001.
[2] T. Nigussie and E. Dribssa, "Design and CFD analysis of centrifugal pump," International Journal of Engineering Research and General Science, vol. 3, pp. 668-677, 2015.
[3] M. H. Ismail, "Design and development of centrifugal pump impeller for performance enhancement."
[4] D. Li, "Numerical Simulation of Internal Flow Field of Centrifugal Fan for Clearing and Selecting Grain Harvester," Journal of Engineering Mechanics and Machinery, vol. 5, pp. 12-18, 2020.
[5] Y. Galerkin and A. Drozdov, "Centrifugal compressor stage design principles checking," in Gas Turbine India Conference, 2015, p. V001T01A006.
[6] S. Shanmukhan and B. Binulal, "Numerical study of a regenerative centrifugal pump," in 2016 International Conference on Energy Efficient Technologies for Sustainability (ICEETS), 2016, pp. 694-698.
[7] E. Franco-Lara, "Enabling Technologies: Fermentation and Downstream Processing," White Biotechnology, vol. 105, p. 205, 2007.
[8] M. Hundshagen, M. Mansour, D. Thévenin, and R. Skoda, "Numerical investigation of two-phase air-water flow in a centrifugal pump with closed or semi-open impeller," in 13 th European Conference on Turbo-machinery Fluid dynamics & Thermodynamics, 2019.
[9] P. AmitKumar, K. K. Jain, R. KDave, and A. Choudhary, "CFD analysis of centrifugal pump impeller having different exit blade width, exit diameter and trailing edge blade angle to enhance performance," 2017.
[10] J. M. Sorokes and M. J. Kuzdzal, "A review of aerodynamically induced forces acting on centrifugal compressors, and resulting vibration characteristics of rotors," in Proceedings of the 50th Turbo-machinery Symposium, 2021.
[11] O. Hamomd, X. Tian, Z. Chen, A. Abdulrahman, F. Gu, and A. Ball, "A new method of vibration analysis for the diagnosis of impeller in a centrifugal pump," 2014.
[12] S. Guo and Y. Maruta, "Experimental investigations on pressure fluctuations and vibration of the impeller in a centrifugal pump with vaned diffusers," JSME International Journal Series B Fluids and Thermal Engineering, vol. 48, pp. 136-143, 2005.
[13] H. Sun, S. Yuan, and Y. Luo, "Cyclic spectral analysis of vibration signals for centrifugal pump fault characterization," IEEE Sensors Journal, vol. 18, pp. 2925-2933, 2018.
[14] G. Mousmoulis, N. Karlsen-Davies, G. Aggidis, I. Anagnostopoulos, and D. Papantonis, "Experimental analysis of cavitation in a centrifugal pump using acoustic emission, vibration measurements and flow visualization," European Journal of Mechanics-B/Fluids, vol. 75, pp. 300-311, 2019.
[15] M. Jahangiri and S. A. Seyed Roknizadeh, "Clogged impeller diagnosis in the centrifugal pump using the vibration and motor current analysis," Journal of Applied and Computational Mechanics, vol. 4, pp. 310-317, 2018.
[16] Y. Yang, L. Zhou, H. Zhou, W. Lv, J. Wang, W. Shi, et al., "Optimal design of slit impeller for low specific speed centrifugal pump based on

orthogonal test," Journal of Marine Science and Engineering, vol. 9, p. 121, 2021.
[17] W. Abdulkarem, R. Amuthakkannan, and K. F. Al-Raheem, "Centrifugal pump impeller crack detection using vibration analysis," in 2nd International Conference on Research in Science, Engineering and Technology, 2014, pp. 206-211.
[18] M. Irfan and A. Glowacz, "Design of a novel electric diagnostic technique for fault analysis of centrifugal pumps," Applied Sciences, vol. 9, p. 5093, 2019.
[19] E. Rusiński, P. Moczko, P. Odyjas, and D. Pietrusiak, "Investigation of vibrations of a main centrifugal fan used in mine ventilation," Archives of Civil and Mechanical Engineering, vol. 14, pp. 569-579, 2014.
[20] M. Ashri, S. Karuppanan, S. Patil, and I. Ibrahim, "Modal analysis of a centrifugal pump impeller using finite element method," in MATEC web of conferences, 2014, p. 04030.
[21] H. Liu, J. Ding, H. Dai, M. Tan, and X. Tang, "Numerical research on hydraulically generated vibration and noise of a centrifugal pump volute with impeller outlet width variation," Mathematical problems in Engineering, vol. 2014, 2014.
[22] A. R. Mohanty, P. K. Pradhan, N. P. Mahalik, and S. G. Dastidar, "Fault detection in a centrifugal pump using vibration and motor current signature analysis," International Journal of Automation and Control, vol. 6, pp. 261-276, 2012.
[23] V. Ramamurti, D. Subramani, and K. Sridhara, "Free vibration analysis of a turbocharger centrifugal compressor impeller," Mechanism and machine theory, vol. 30, pp. 619-628, 1995.
[24] S. Lemeš and N. Zaimović-Uzunović, "Mode shapes of centrifugal pump impeller," in Proceedings of the 6th International Research/Expert Conference on Trends in the Development of Machinery and Associated Technology (TMT 2002), Neum, Bosnia and Herzegovina, 2002, pp. 18-22.
[25] W. Zhao, J. Ge, D. Ma, C. Li, and S. Bao, "Vibration analysis of large centrifugal pump rotors," in IOP Conference Series: Materials Science and Engineering, 2013, p. 022033.
[26] N. Sakthivel, V. Sugumaran, and S. Babudevasenapati, "Vibration based fault diagnosis of monoblock centrifugal pump using decision tree," Expert Systems with Applications, vol. 37, pp. 4040-4049, 2010.
[27] S. Farokhzad, "Vibration based fault detection of centrifugal pump by fast fourier transform and adaptive neuro-fuzzy inference system," Journal of mechanical engineering and technology, vol. 1, pp. 82-87, 2013.
[28] D. Hagelstein, H. Hasemann, and M. Rautenberg, "Coupled vibration of unshrouded centrifugal compressor impellers. Part II: computation of vibration behavior," International Journal of Rotating Machinery, vol. 6, pp. 115-128, 2000.
[29] M. P. Singh, B. K. Thakur, W. E. Sullivan, and G. Donald, "Resonance Identification For Impellers," in Proceedings of the 32nd Turbo-machinery Symposium, 2003.
[30] A. A. Pinheiro, I. M. Brandao, and C. Da Costa, "Vibration analysis in turbomachines using machine learning techniques," European Journal of Engineering and Technology Research, vol. 4, pp. 12-16, 2019.
[31] F. E. Selamat, W. H. I. Wan Izhan, and B. S. Baharudin, "Design and Analysis of centrifugal pump impeller for performance enhancement," Journal of Mechanical Engineering (JMechE), pp. 36-53, 2018.
[32] T. Capurso, L. Bergamini, S. M. Camporeale, B. Fortunato, and M. Torresi, "CFD analysis of the performance of a novel impeller for a double suction centrifugal pump working as a turbine," in 13 th European Conference on Turbo-machinery Fluid dynamics & Thermodynamics, 2019.
[33] K. K. Yadav, K. Mendiratta, and V. Gahlot, "Optimization Of Design Of Mixed Flow Centrifugal Pump Impeller Using Cfd," International Journal of Research in Engineering and Technology, ISSN, pp. 2319-1163, 2016.
[34] L. J. Sadik, Enhancing Centrifugal Pump Performance by Adding Cylindrical Disks at the Impeller Inner Suction: Lawrence Technological University, 2020.
[35] K. K. Yadav and V. Gahlot, "Performance improvement of mixed flow pump impeller through CFD analysis," International Journal of Research in Engineering and Technology, vol. 4, pp. 243-247, 2015.
[36] A. Albraik, F. Althobiani, F. Gu, and A. Ball, "Diagnosis of centrifugal pump faults using vibration methods," in Journal of Physics: Conference Series, 2012, p. 012139.
[37] A. Shooshtari, M. Karimi, M. Shemshadi, and S. Seraj, "Effect of impeller diameter on dynamic response of a centrifugal pump rotor," Vibration, vol. 4, pp. 117-129, 2021.
[38] A. R. Al-Obaidi, "Investigation of effect of pump rotational speed on performance and detection of cavitation within a centrifugal pump using vibration analysis," Heliyon, vol. 5, 2019.
[39] Y. Yuan, S. Yuan, and L. Tang, "Investigation on the effect of complex impeller on vibration characteristics for a high-speed centrifugal pump," Proceedings of the Institution of Mechanical Engineers, Part A: Journal of Power and Energy, vol. 234, pp. 611-624, 2020.
[40] B. Qian, P. Wu, B. Huang, K. Zhang, S. Li, and D. Wu, "Optimization of a centrifugal impeller on blade thickness distribution to reduce hydro-induced vibration," Journal of Fluids Engineering, vol. 142, p. 021202, 2020.
[41] S. Wang, Y. Zi, B. Li, C. Zhang, and Z. He, "Reduced-order modeling for mistuned centrifugal impellers with crack damages," Journal of Sound and Vibration, vol. 333, pp. 6979-6995, 2014.
[42] X. Zhao, Q. Zhou, S. Yang, and H. Li, "Rotating stall induced non-synchronous blade vibration analysis for an unshrouded industrial centrifugal compressor," Sensors, vol. 19, p. 4995, 2019.
[43] M. Oza and D. Shah, "Theoretical and experimental modal analysis of centrifugal pump radial flow impeller," in IOP Conference Series: Materials Science and Engineering, 2020, p. 012003.
[44] H. Han, S. Jeon, C. Lee, and Y. Kim, "Self-excited vibration of an impeller blade of the waterjet propulsion shaft in a naval vessel caused by flow-induced thrust load," Engineering Failure Analysis, vol. 118, p. 104888, 2020.